Thesis for the Degree of Master of Engineering

Development of LED Face Mask with Optimal Power Consumption and Power Density Control using Fuzzy Logic Controller

By

Phan Duc Tri

Department of Interdisciplinary Program of Biomedical Mechanical and Electrical Engineering

The Graduate School

Pukyong National University

February 2020

Development of LED Face Mask with Optimal Power Consumption and Power Density Control using Fuzzy Logic Controller

(퍼지 로직 컨트롤러를 이용한 최적 소비전력 및 에너지 밀도 제어 기능을 갖춘 LED 마스크 개발)

Advisor: Prof. Junghwan Oh

by

Phan Duc Tri

A thesis submitted in partial fulfillment of the requirements for the degree of

Master of Engineering

In Department of Interdisciplinary Program of Biomedical Mechanical and Electrical Engineering

Graduate School

Pukyong National University

February 2020

Development of LED Face Mask with Optimal Power Consumption and Power Density Control using Fuzzy Logic Controller 퍼지 로직 컨트롤러를 이용한 최적 소비전력 및 에너지 밀도 제어 기능을 갖춘 LED 마스크 개발

A dissertation

By

Phan Duc Tri

Approved by:

(Chairman) Prof. Seung Yun Nam, Ph.D.

(Member) Prof. Joong Ho Shin, Ph.D

(Member) Prof. Junghwan Oh, Ph.D.

January 2020

LIST OF CONTENTS

Development of LED Face Mask with Optimal Power Consumption and Power Density Control using Fuzzy Logic Controller

Phan Duc Tri

Department of Interdisciplinary Program of Biomedical Mechanical and Electrical Engineering,
The Graduate School, Pukyong National University

Abstract

발광 다이오드 (LED) 페이스 마스크의 생물학적 효과는 주로 파장 및 전력 밀도의 조사 파라미터에 의해 결정된다. 그러나 배터리를 사용하여 전력을 공급하는 것은 배터리 방전 동안 LED 전력 밀도의 변화에 문제를 일으킨다. 결과적으로 배터리 수명 연장 및 작동 시간 연장과 함께 안정적인 LED 전력 밀도를 유지하는 것이 LED 페이스 마스크의 설계에서 주요 관심사이다. 본 연구는 낮은 에너지 소비 및 일정한 전력 밀도 제어를 갖는 LED 페이스 마스크의 설계를 소개하는 것을 목표로 한다. 전력 소비 최적화는 작동 시간이 22% 증가한 하드웨어 및 소프트웨어 공동 설계를 통해 달성되었습니다. 정 전력 밀도 제어와 관련하여, LED 전력 밀도와 동작 시간 사이의 관계에 기초한 퍼지 로직이 제안되었다. 검증 결과 새로 설계된 컨트롤러에 대해 최소 40 분의 40mW/cm2 전력 밀도에서 60 분 동안 작동하는 LED 페이스 마스크의 전력 밀도가 최소 오류 (각각 녹색, 청색 및 적색 광선의 경우 1.3, 3.3, 1.5 %)로 확인되었습니다. 새롭게 설계된 LED 페이스 마스크는 광범위한 전압 변동에서 에너지 절약 및 안정된 LED 전력 방출 특성을 갖춘 고급 버전으로 간주 될 수 있습니다.

Keywords: LED power density control; LED face mask; Fuzzy logic; low power consumption.

LIST OF TABLE

LIST OF FIGURES

Chapter 1. Introduction

In present days, the management of dermatological diseases, skin rejuvenation and aesthetic treatment involves the use of topical and systemic antibiotics, retinoids and chemical peelings [1-4]. However, the increased risk of bacterial resistance in antibiotic therapy and the adverse effects of retinoid therapy is causing skin irritation and deterioration are widely documented [5-7]. In recent years, LED phototherapy has been emerged as a safe and side effect-free therapy for skin diseases and skin rejuvenation [8]. The efficacy of LED phototherapy in reducing pain and inflammation, tissue augmentation, promoting regeneration have been reported in some studies. For instance, the efficacy of blue and red LED combination in improving skin tone, skin texture and reduced melanin level has been proved [9]. Goldberg et al [10] investigated the efficacy of LED therapy with 415 nm and 633 nm wavelength in mild inflammatory lesion and acne treatment. According to the above researches, providing an appropriate wavelength, LED power density and an adequate standard dose could be seen as main factors, which determines the success of LED phototherapy treatment [11].

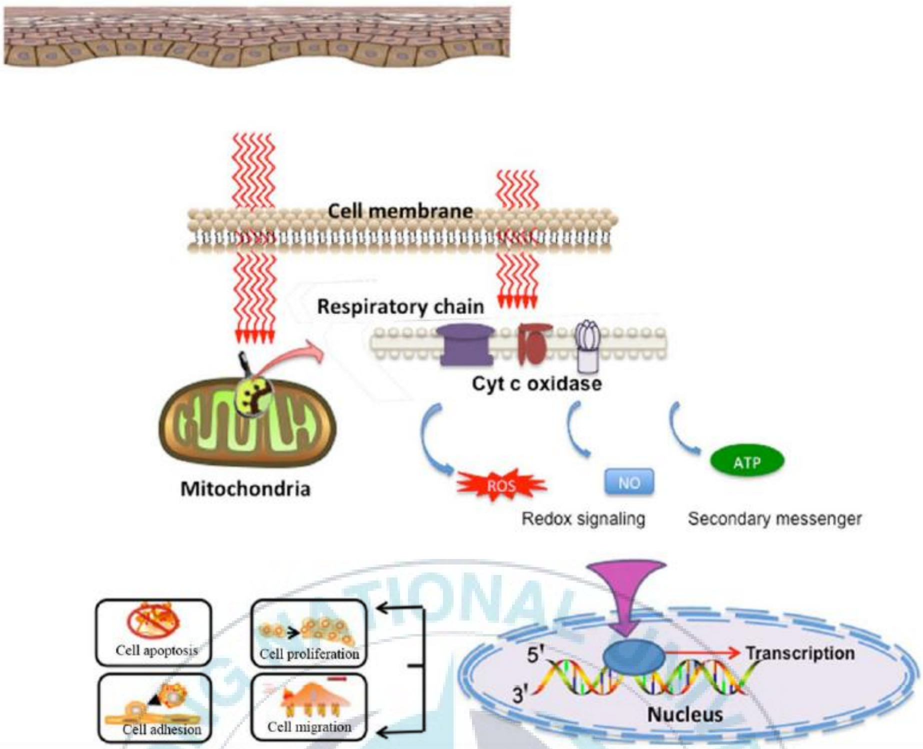

Figure 1 Mechanism of action of LLLT [1]

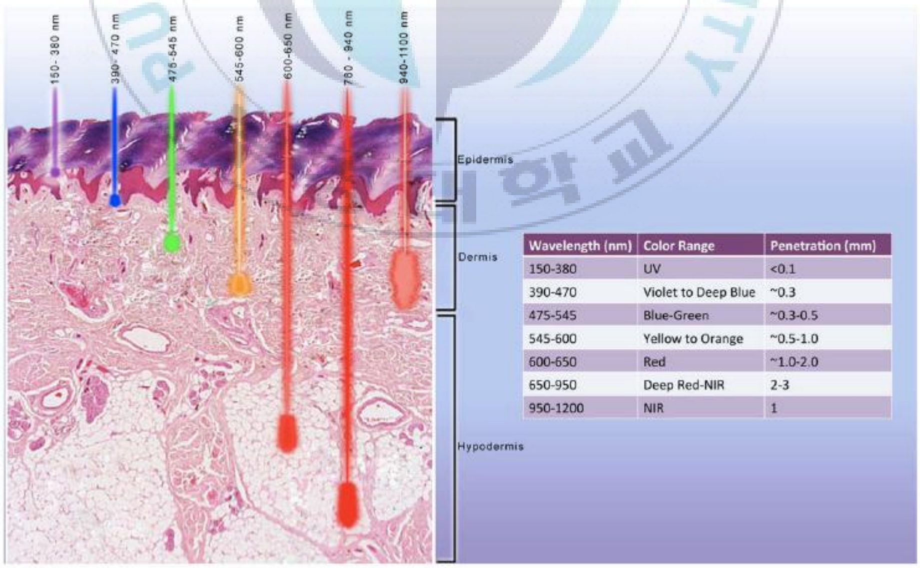

Wavelength (nm)	Color Range	Penetration (mm)
150-380	UV	<0.1
390-470	Violet to Deep Blue	~0.3
475-545	Blue-Green	~0.3-0.5
545-600	Yellow to Orange	~0.5-1.0
600-650	Red	~1.0-2.0
650-950	Deep Red-NIR	2-3
950-1200	NIR	1

Figure 2 Tissue penetration depths of various wavelengths [1]

Table 1 Examples of LLLT Devices for Dermatological Applications [1]

Supplier	Wavelength (nm)	Power Density	Standard Dose	Application
PhotoMedex (Manchester, UK)	415 (±5) 633 (±6)	40 105	48 126	Acne, photo-damage, non-melanoma skin cancers, skin rejuvenation, vitiligo and wound healing post elective surgery
Edge Systems (Signal Hill, CA)	600–700		7.4 J per treatment area	Acne, improving skin texture, firmness and resilience, increasing lymphatic system activity, fine lines, wrinkles and superficial hyperpigmentation
Flip 4 (Sainte-Julie, Quebec, Canada)	420–700	≤4		Acne, rejuvenation, injured skin healing including the shortening of the post skin resurfacing erythema duration
Light BioSciences (Virginia Beach, VA)	588 (±10)	Variable		Anti-aging

OPUSMED (Montreal, Canada)	660	150		Anti-aging
Revitalight (Chicago, IL)	420 590	80 80	7.2 J per 90 sec. per treatment area	Fine lines, wrinkles, and age spots on the face, neck and hands
Soli-Tone (Woburn, MA)	470 525			Acne, anti-aging, hyperpigmentation, rosacea
DUSA (Wilmington, MA)	417	10		Acne
Curelight (Rehovot, Israel)	405–420		60	Acne, anti-aging, skin rejuvenation, acceleration of healing of post peel and post surgical suture sites
Lumenis (Santa Clara, CA)	405–420	200	60	Acne

However, similar to other wearable and battery-operated devices, the LED phototherapy devices also encounter a challenge of stabilizing LED power density under the variation of battery voltage. The variable characteristics and parameters could cause undesirable effects on skin treatment as well as decrease the reliability of this device. In this present study, we developed a low power consumption LED face mask with constant-power control system using Fuzzy logic controller to control LED power density.

The energy optimization of LED face mask was achieved by separating multiple power modules and activating low power mode in each main component. For instance, 1.9 V voltage was supplied for both PIC16LF19186 [12] and Bluetooth modules RN4020 [13], 3.3 V power supply was provided for PCA 9956 LED [14]. The optimization in power consumption lead to increasing the operating capability of LED face mask battery and improving the accuracy of LED power density [15].

A lot of commercial DC/DC converter with constant-current and voltage output are widely used in LED system to maintain LED power. However, the energy conversion loss and adaptability of DC/DC power converter in controlling LED color and LED power cause problems in using for LED phototherapy system [16]. The purpose of this paper is to introduce a LED power density control system with Fuzzy logic controller based on the relationship between LED power density and operating time [17-20]. Additionally, the proposed system is composed of an IoT (internet of Things) controlling system that uses a smartphone application with Android, Windows and IOS to provide users with a satisfactory LED power density and daily phototherapy dose [21, 22]. Furthermore, the history of phototherapy regimen and LED dose for treatment could be monitored and saved for diagnosis and prognosis.

Chapter 2. DESIGN OF LED FACE MASK WITH LOW POWER CONSUMPTION

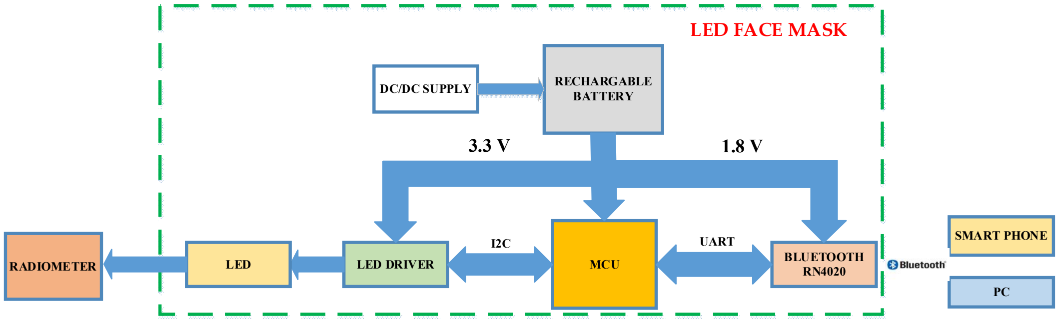

Figure 3 The block diagram of the proposed LED face mask

The design of LED face mask system is demonstrated in Fig. 3. In this design, red (635 nm), green (515 nm) and blue (413 nm) LED from Wurth Elektronik, Germany [23] were selected and LED driver PCA9956 from NXP Semiconductors, Netherland [14] was used to control the LED light source. LED power density can be controlled from 0-40 mW/cm^2, 0-100 mW/cm^2, 0-60 mW/cm^2 for red, blue and green LED, respectively. The proposed LED face mask design was divided into four main modules. The first module is the power module which consists of a rechargeable battery, an integrated host-controlled Li-ion BQ24130 [24] and a low power voltage converter TPS 76318 [25] and TPS 613221 [26]. The second one is the LED controller module with the use of a low power LED driver [14]. The third module is Bluetooth Low Energy (BLE) module RN4020 [13]. The final module is microcontroller (PIC 16LF19186) with the advantage of extreme low power (XLP) function [12].

As schematized in Fig. 3, a smart phone application or a personal computer (PC) via Bluetooth is used to control the LED color, LED power density and treatment time of LED face mask. The data from dose and history of therapy treatment can be collected and saved by the Apps for further diagnosis and monitoring the efficacy of LED phototherapy on dermatological treatment. The proposed hardware design of LED face mask and LED face mask controller is shown in Fig. 4 and Fig. 5, respectively.

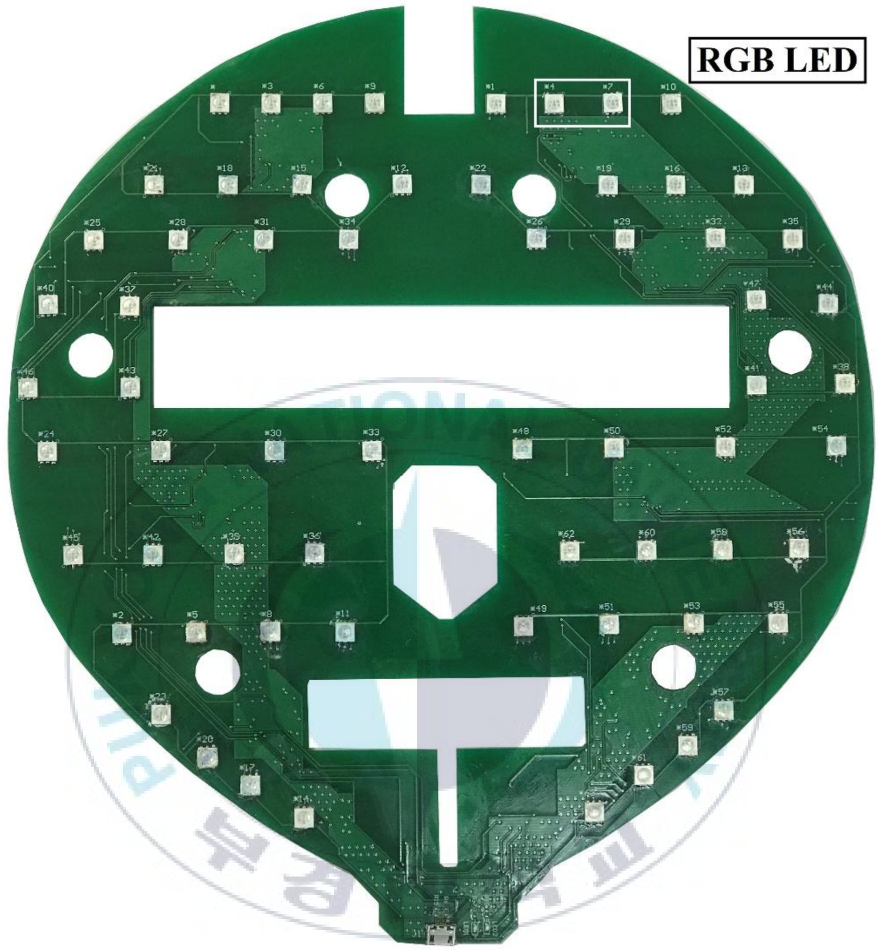

(a)

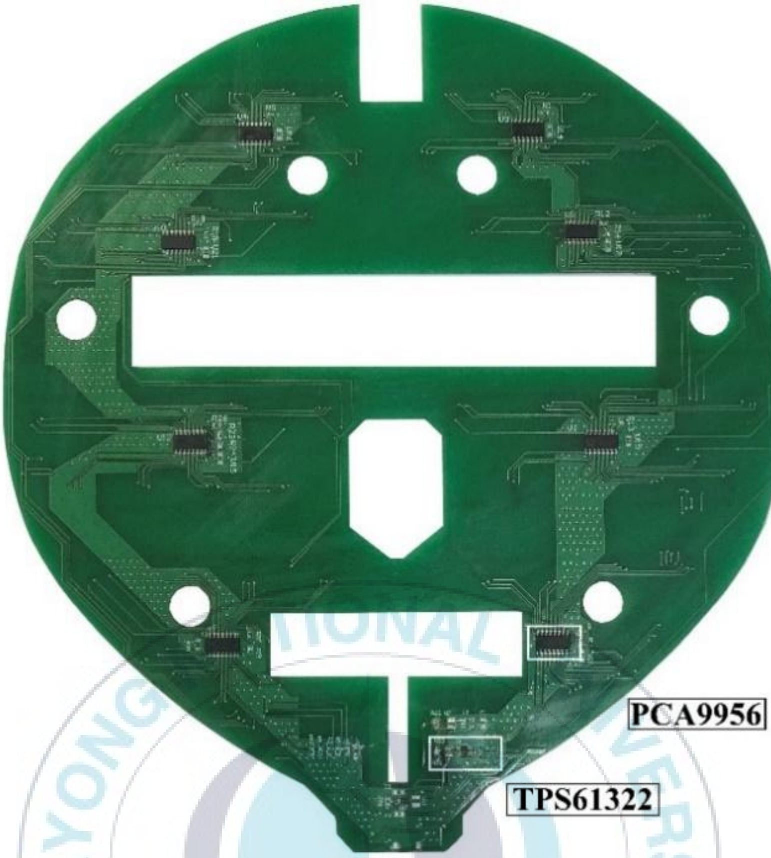

(b)

Figure 4 The prototype of LED face mask (a) front side and (b) back Side

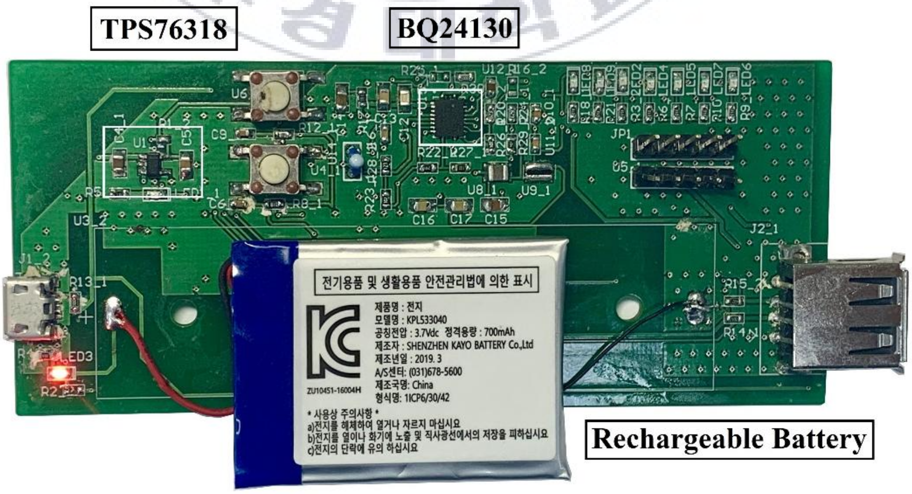

(a)

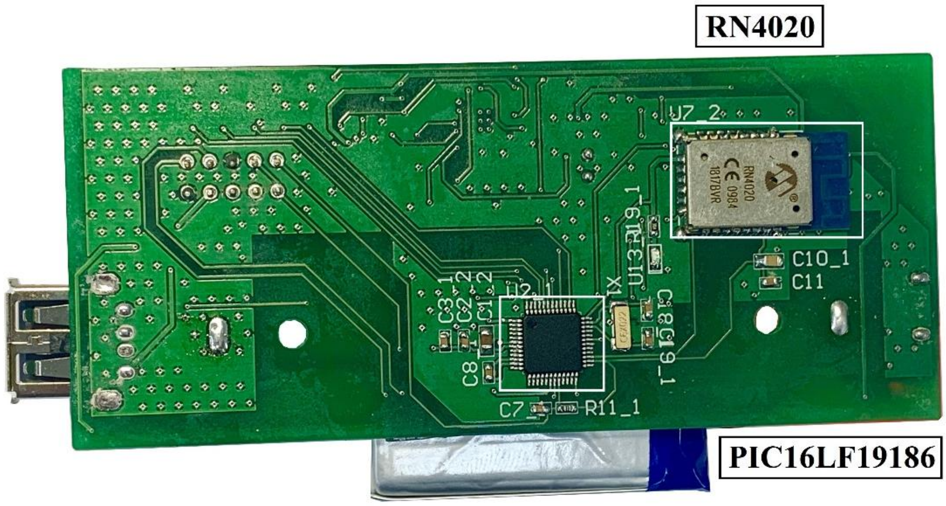

(b)

Figure 5 The PCB design of LED face mask controller (a) front side and (b) back side

1. Printed Circuit Board (PCB) Design

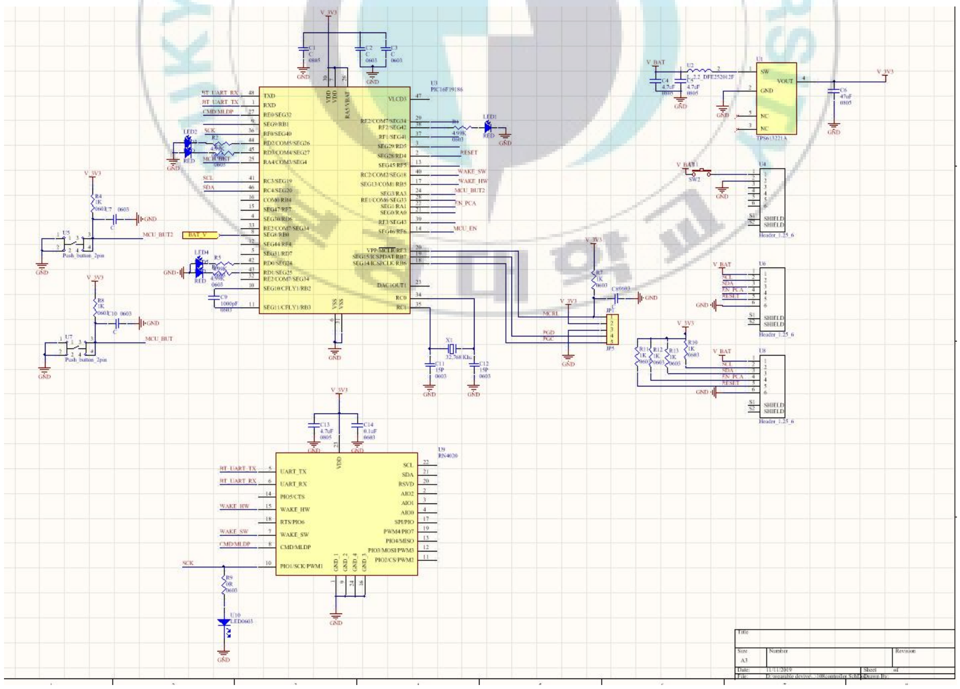

Figure 6 Controller schematic

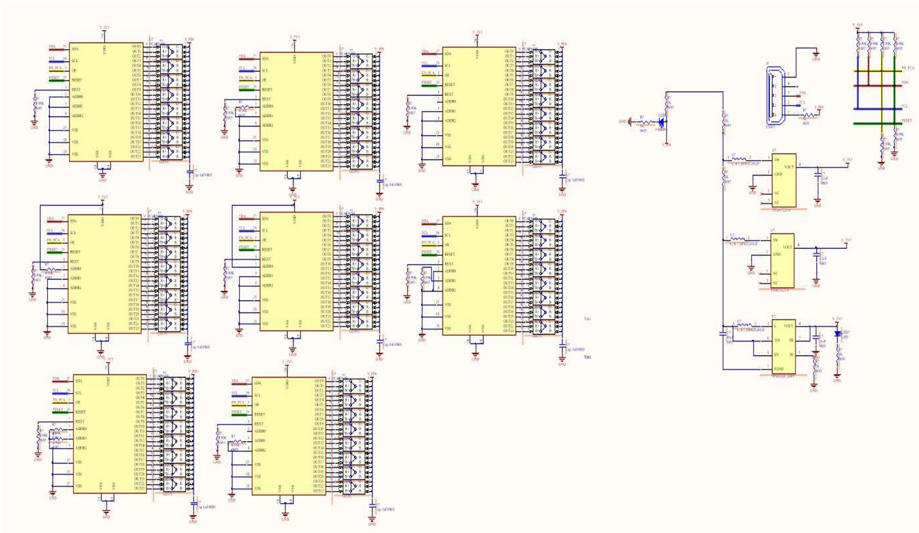

Figure 7 LED face mask schematic

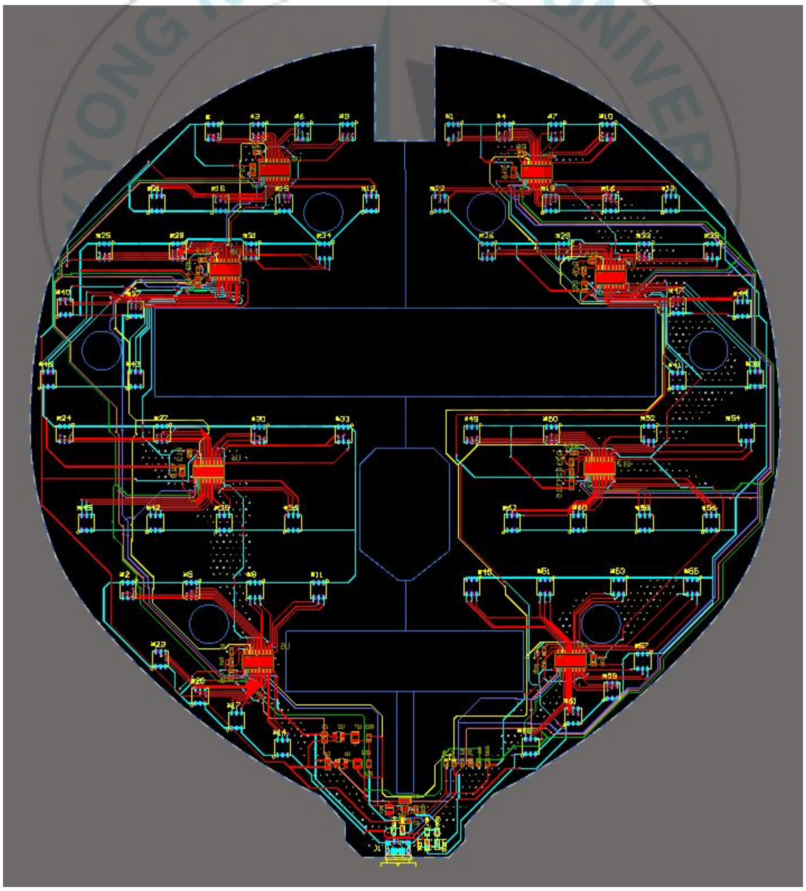

Figure 8 The PCB design of LED face mask

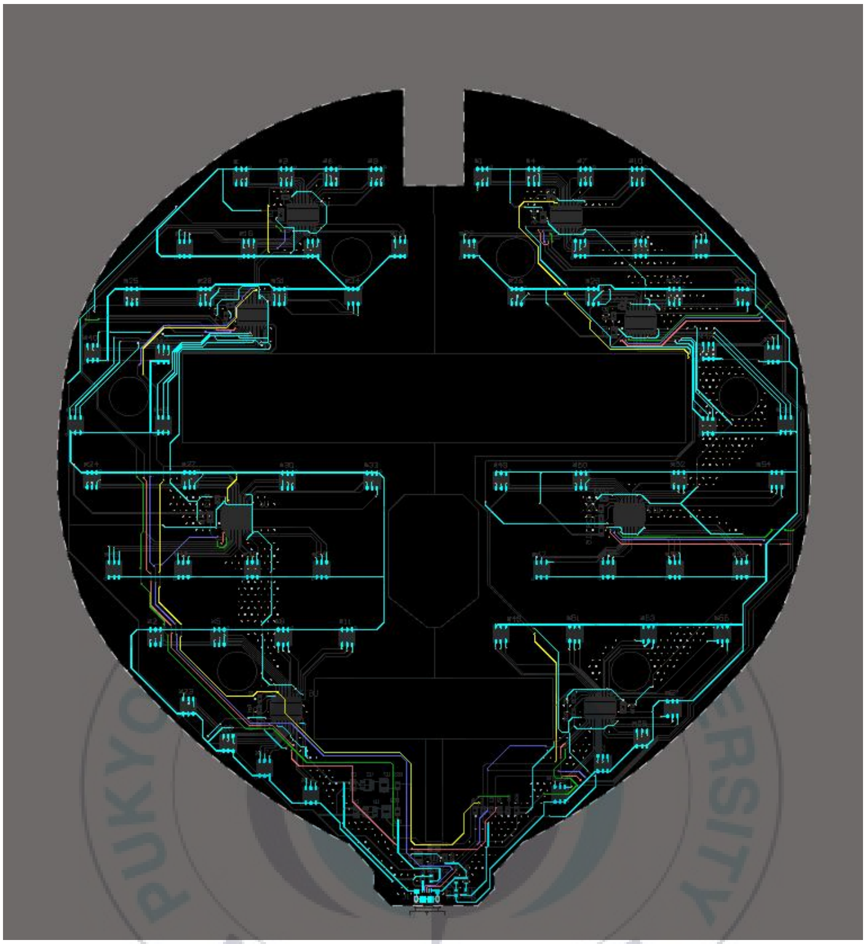

Figure 9 The top layer of LED face mask

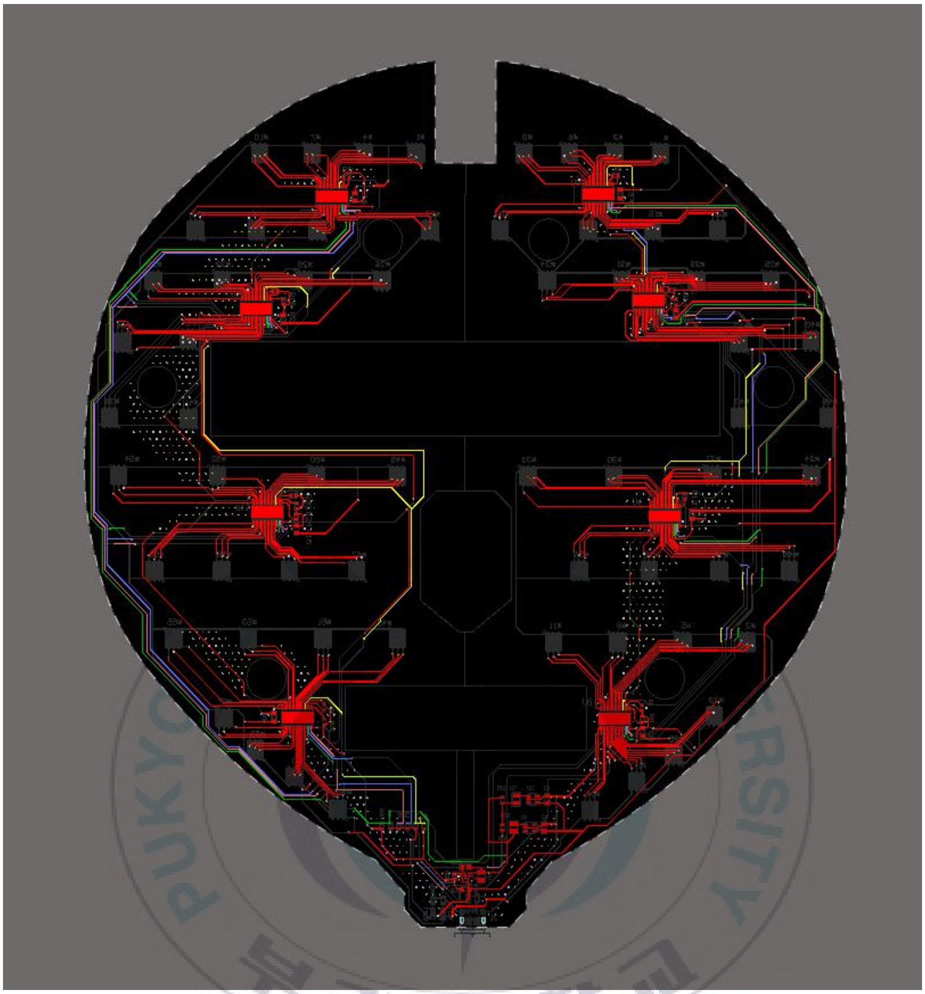

Figure 10 The bottom layer of LED face mask

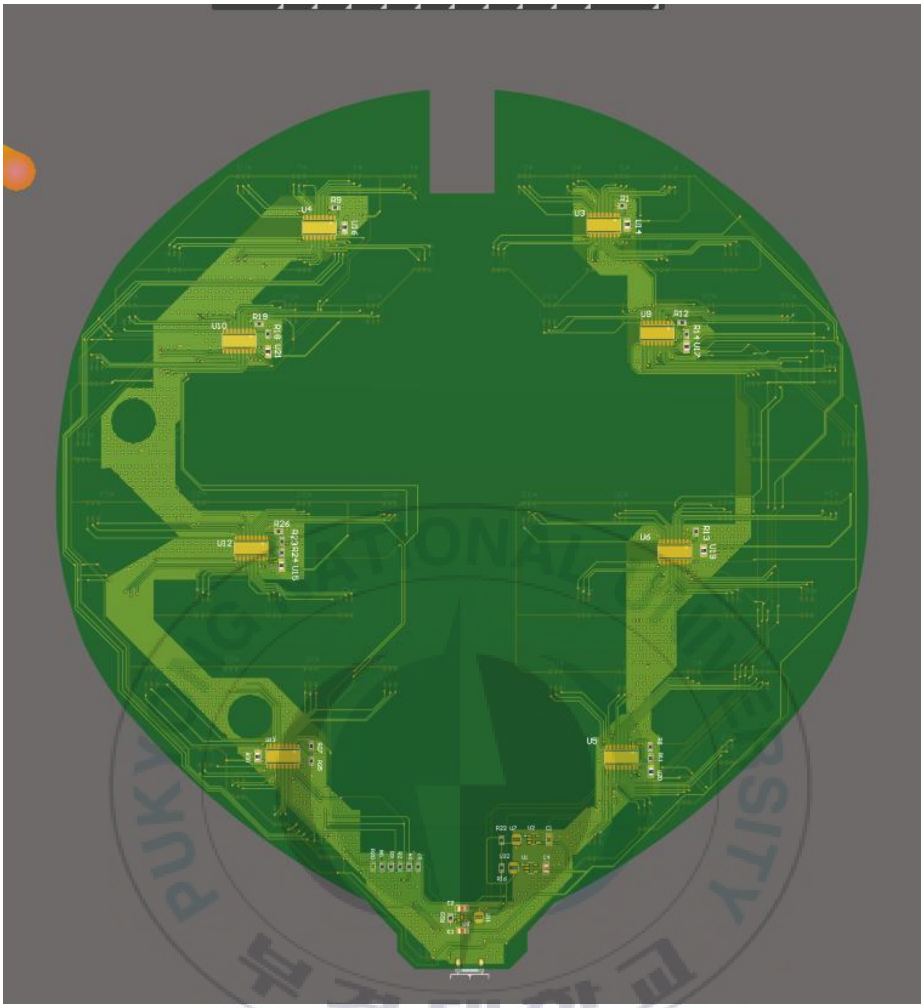

Figure 11 The 3D top layer of LED face mask

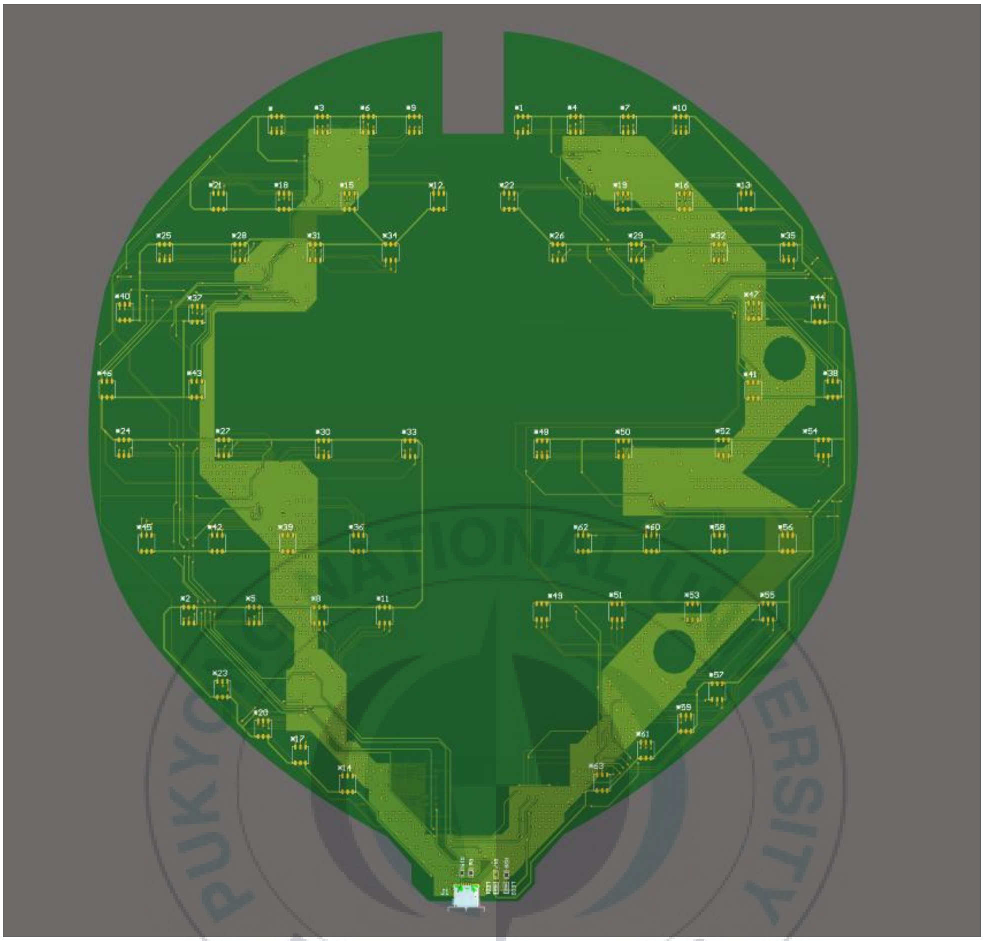

Figure 12 The 3D bottom layer of LED face mask

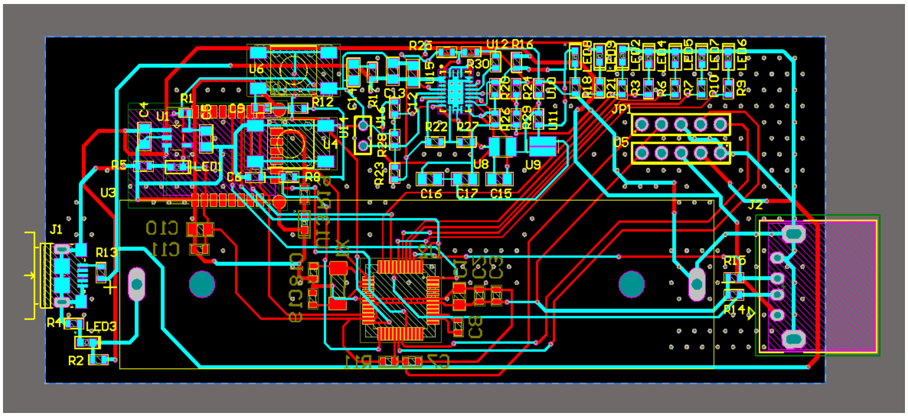

Figure 13 The PCB design of controller

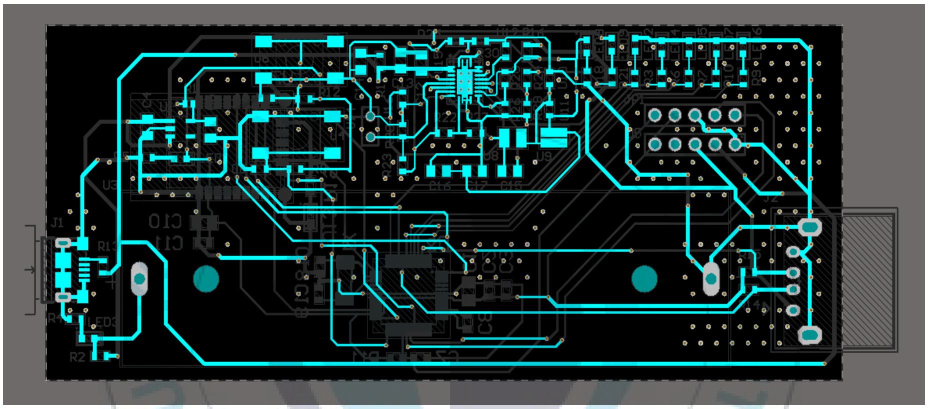

Figure 14 The top layer of controller

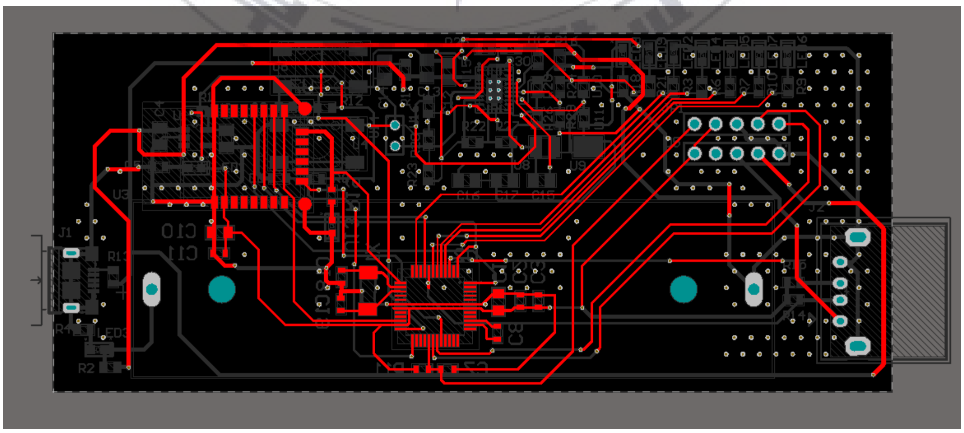

Figure 15 The bottom layer of controller

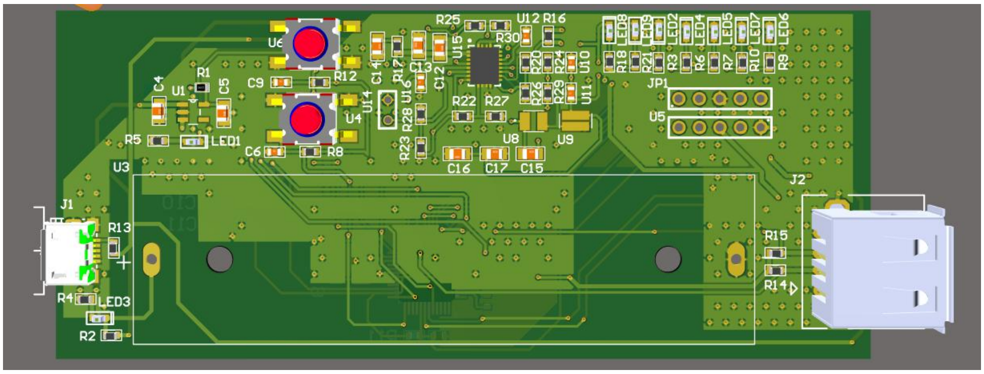

Figure 16 The 3D top layer of controller

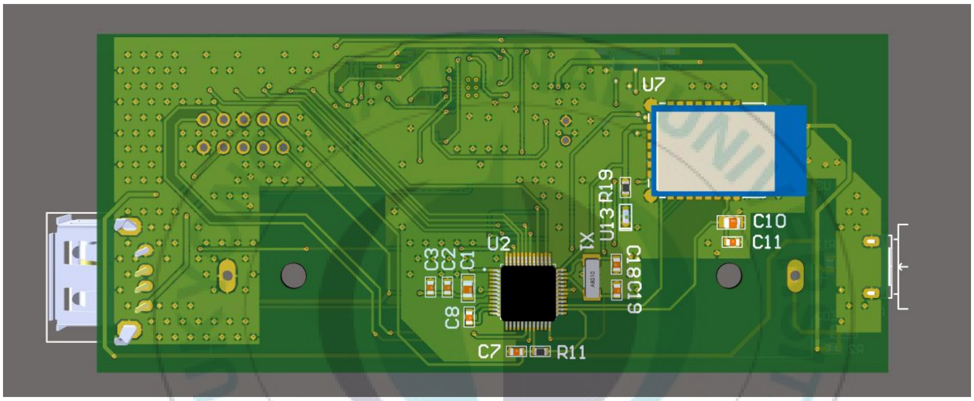

Figure 17 The 3D top layer of controller

Altium Designer software was also used to design the printed circuit board. The PCB of LED face mask system was designed in two layers with both two kinds of electrical components (the surface mounted and through holes). The 2D, 3D and real image of the circuit was shown.

2. Low Power Hardware Design

2.1. Lower Module Design

According to the manufacturer's datasheet, the operating voltages and current consumption of the three main components (PIC 16LF19186, PCA 9956 and RN 4020) were shown in Table 2.

Table 2 Operating voltage and current of three devices PCA 9956, RN4020, PIC16LF19186

Components	Operating Voltage (V)	Operating Current (μA)
PIC16LF19168	1.8-3.6	Sleep mode 50nA@1.8V
		Active mode 8μA/ 32kHz @1.8V
		Active mode 32μA/ MHz @1.8V
		Second OSC 500na@32kHz
RN4020	1.8-3.6	Dormant < 900nA @3V
		Deep Sleep < 5.0μA@3V
		Idle <1.5 mA@3V
		TX/ RX Active 16 mA@3V
		TX Power (dBm) -19.1 with 14.0 mA@3.3V
PCA9956	3 - 5.5	LED[23:0] = off: 12 mA@3V
		LED[23:0] = on: 21 mA@3V

TPS76318 [26] are part of low-dropout (LDO) voltage regulators with lower dropout voltage and quiescent currents compared to conventional LDO regulators. The TPS 76318 is based on a PMOS pass element to reduce the quiescent current (140 μA maximum) and constant the output current (0 mA to 150 mA). The supply current could be reduced less than 2 μA when the regulator is in sleep mode. With the advantages of optimization in the low-dropout voltage feature and low-power operation, TPS 76318 was selected for this design.

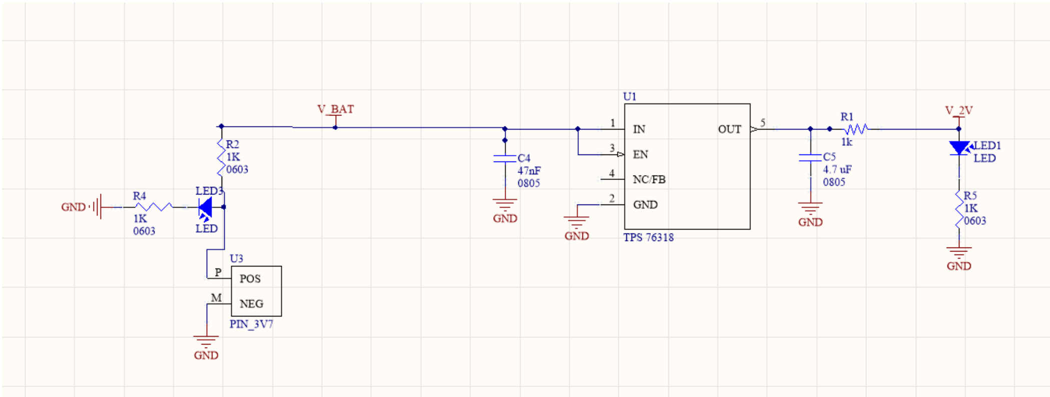

Figure 18 The schematic of TPS76318

With the advantages of high efficiency (up to 96%) and low quiescent current (15 μA), the host-controlled battery charger Bq24130 [24] was chosen in this design. When the input voltage reduces below the battery voltage, the Bq241630 automatically turn on sleep mode to minimize current drain from the battery.

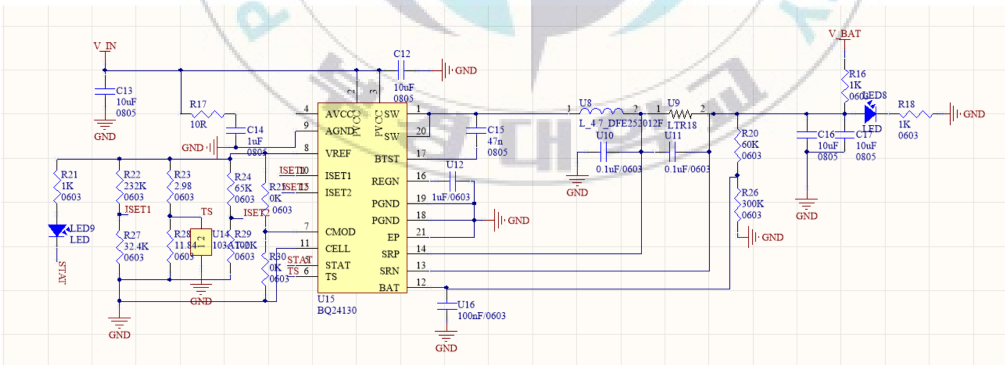

Figure 19 The schematic of Bq24130

Synchronous boost converter TPS613221 [26], with a low quiescent current (6.5 μA) and high efficiency (higher 90%), was designed for this system to provide 3.3 voltage for LED- driver. The input voltage range is from 2.7 V to

3.7 V, and the TPS 613221 can work with the input voltage under 0.4V. With the advantage of a hysteretic control topology using synchronous rectification, the TPS 61322 consume only 6.5-µA quiescent current and achieve higher voltage conversion which results in extending operating time of battery and minimizing the power consumption in this design.

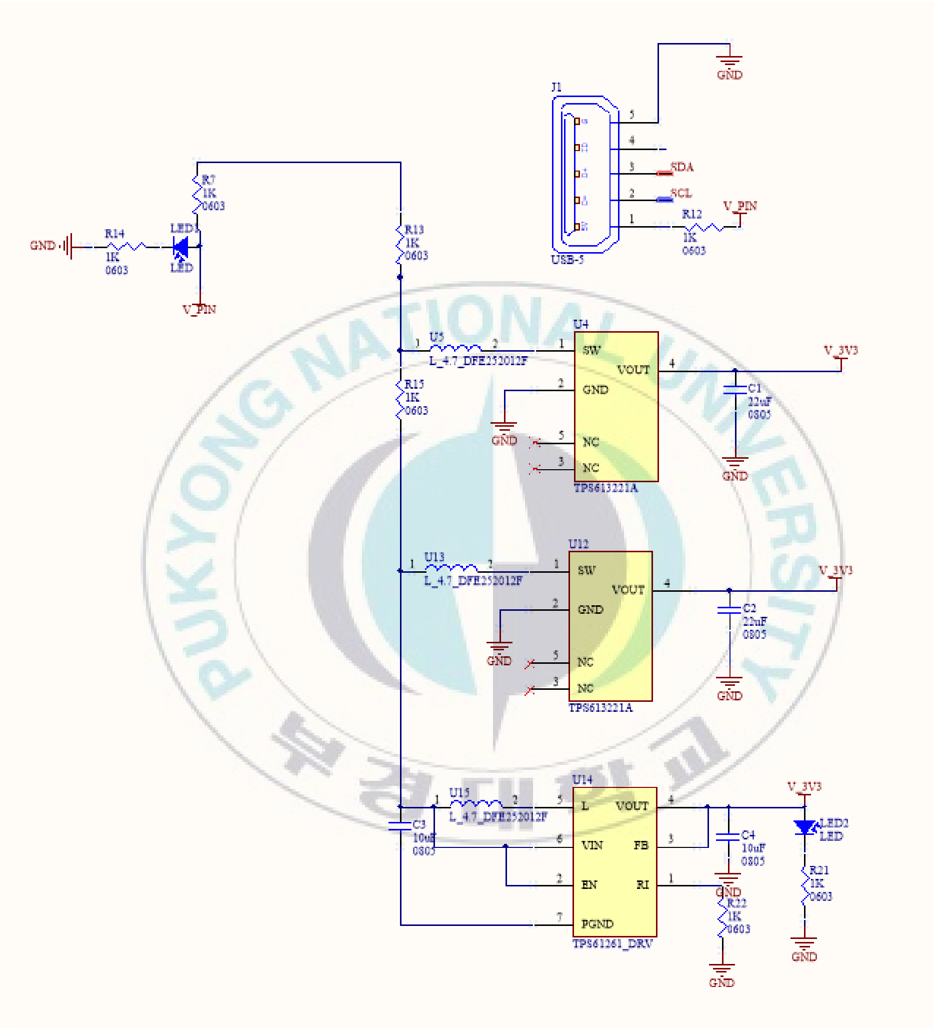

Figure 20 The schematic of TPS 61322

2.2.The Optimization of Power Consumption

In proposed hardware design, the optimization of power consumption was achieved by separating and reducing the voltage of the main components to minimum value. Additionally, an external crystal of 8 MHz with PLL mode (x4) was utilized for MCU because the internal crystal consumes higher current than external crystal [12]. In proposed firmware design, the energy saving mode in PIC 16LF19186 was configured and Microchip Low Energy Data Profile (MLDP) is active with the smallest value (TX power – 19.1 dBm) in the Bluetooth module to consume the smallest current.

Fig. 21 and Fig. 22 show the operation of the main components in different power-saving modes. In power-saving operation, the sleep mode and power saving mode of LED driver, MCU and Bluetooth module are activated. When the data in smart phone Apps has been prepared and transferred, the Bluetooth module and MCU are switched to active mode to read the data and communicate with smartphone Apps. After transferring data to smartphone Apps, the device enter Mode 3. In Mode 3, the Bluetooth module goes into sleep mode, while MCU and LED drive use I2C interface with frequency of 200 kHz to communicate. After LED driver is configured, MCU and Bluetooth module turn into sleep mode, while LED driver is remaining in active mode to control LED. In Mode 4, if face mask receives a reconfiguration command for power density, LED color or operating time from smart phone Apps, the device will turn back into Mode 2 to change LED driver to sleep mode and wake up MCU as well as Bluetooth module from sleep mode to receive new data. Otherwise, if face mask controller receives a turn off command from smartphone Apps, the device will enter Mode 1 to save energy for LED face mask device and wait for new command from smartphone Apps.

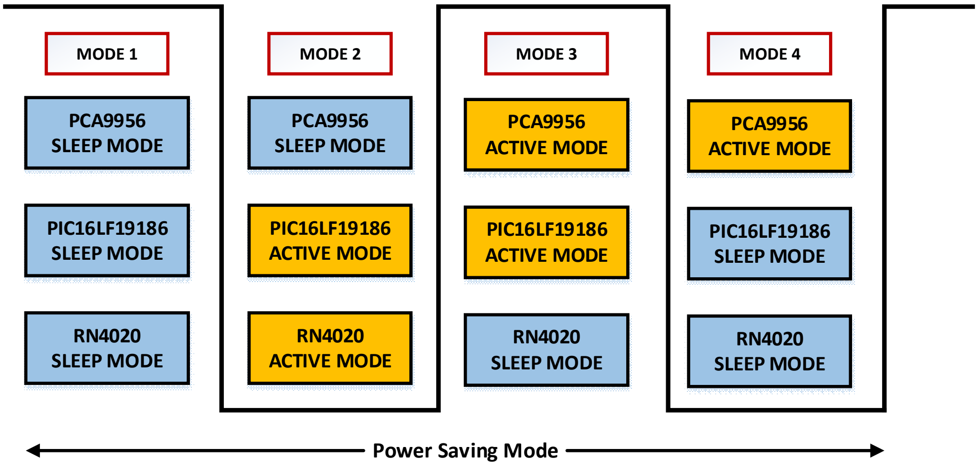

Figure 21 The operation of the proposed LED face mask in power-saving mode.

3. Software Design

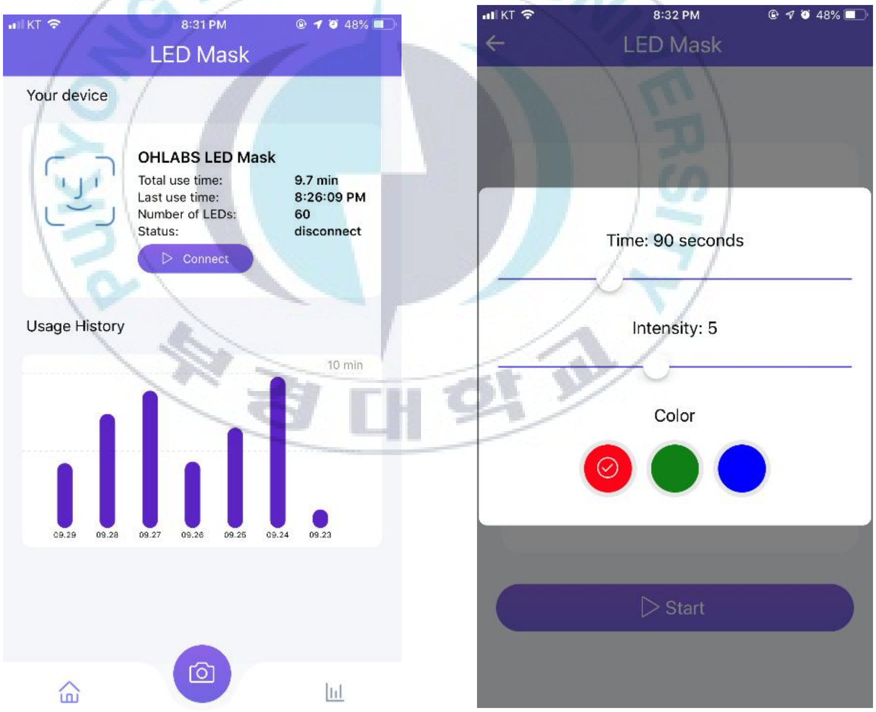

(a) (b)

Figure 22 The smart phone application of LED face mask (a) startup monitor and (b) main monitor

A data package and a data transfer protocol were designed for communication between the smartphone and LED face mask. The data tranfer protocol was used to parses the received data of smart phone. The treatment time, LED power density and LED color (red, green, blue) of the LED face mask was configured by smartphone application.

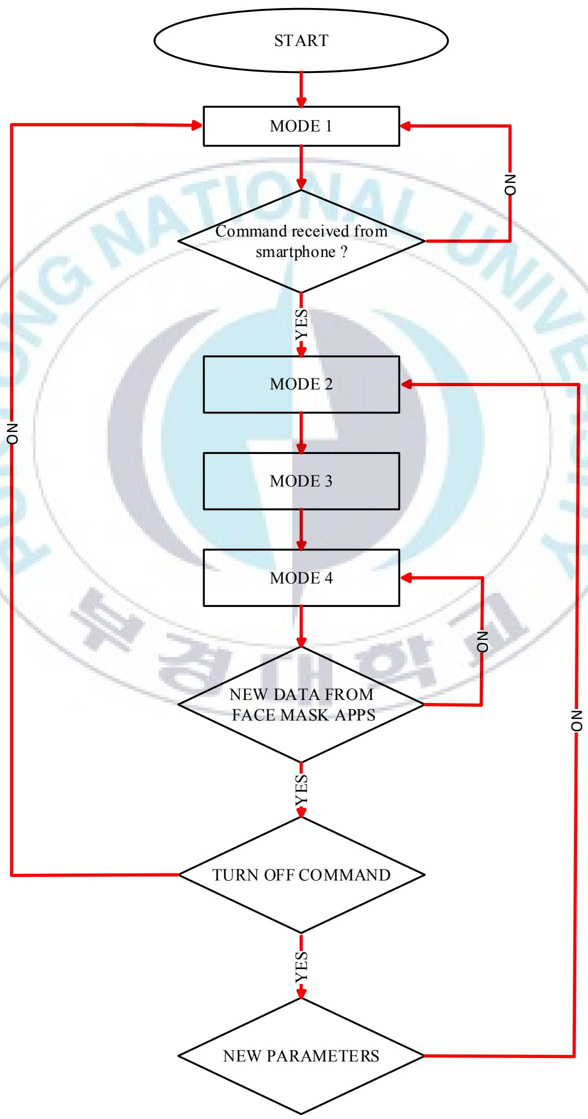

Figure 23 The flow chart of LED face mask operating in power saving mode

4. Experimental Evaluation for optimizing power consumption

In this section, the current consumption of the proposed design at different operating modes and voltage was measured to demonstrate the optimization of power consumption and the increase of operating time in LED face mask. As shown in Section 2.1, the operating voltage of PIC16LF19186, RN4020, PCA9956 was separated and reduced to save energy. Futhermore, sleep mode as well as power saving mode in microcontroller and Bluetooth module were activated to optimize power consumption. In this experiment, RIGOL DP832 and Agilent U3606A power supply were selected to generate 1.8V and 3.3 V. Both the devices are configured with an internal built-in current in order to test the current consumption of the proposed LED face mask design.

Table 3 Current consumption in power saving operation.

Mode	**Status**	**Current Consumption (mA)**
1	Sleep (PIC, RN4020, PCA9956)	0.11
2	Active (PIC, RN4020), Sleep (PCA9956)	3.1
3	Active (PIC, PCA9956), Sleep (RN4020)	161.6
4	Active (PCA9956), Sleep (PIC,RN4020)	160.05

Table 3 shows the current consumption of MCU, LED driver and Bluetooth module in different power saving mode. The current increased markedly from 0.11 mA in mode 1 to 3.1 mA in Mode 2 when PIC and RN 4020 were active. Otherwise, there were a significant change in current consumption from 3.1 mA to 161.6 mA when the device turned into Mode 3. This could be explained by the fact that LED drivers consume the largest proportion of current in the proposed design. While when the device transferred from Mode 3 to Mode 4, the power consumption decreased slightly from 161.6 mA to 160.05 mA due to PIC and RN 4020 in sleep mode. The results indicated that LED drivers are mainly consuming the currents. It is also observed that the current of PIC and RN4020 is smaller compared to LED driver. However, activating sleep mode and reducing voltage in PIC, RN4020 are necessary to optimize current consumption and to increase the operating time of LED face mask.

Table 4 Current consumption in typical operation

Mode	Status	Current Consumption (mA)
1	Active (PCA9956, PIC, RN4020)	173.15

In another test, we also measured the performance of LED face mask in typical operation at 3.3 volts of PIC, RN4020 in active mode to compare the current consumption with the energy-saving operation. According to Table 3 and Table 4, we can see the decrease in current consumption when operating in the power-saving operation and typical operation.

Furthermore, we conducted battery testing to evaluate the energy consumption and the operating capability of battery. The operating time of the LED face mask with the energy-saving operation and the typical operation are shown in Table 5. As a result, the decrease of current and power consumption increased the operating time of LED face mask by approximately 22%.

Table 5 The operating time in saving-energy operation and typical operation

Number	Operation Mode	Used Time (min)
1	Power-saving Mode	86
2	Typical Mode	67

Chapter 3. LED POWER DENSITY WITH FUZZY LOGIC CONTROLLER

1. LED light Power Density control system

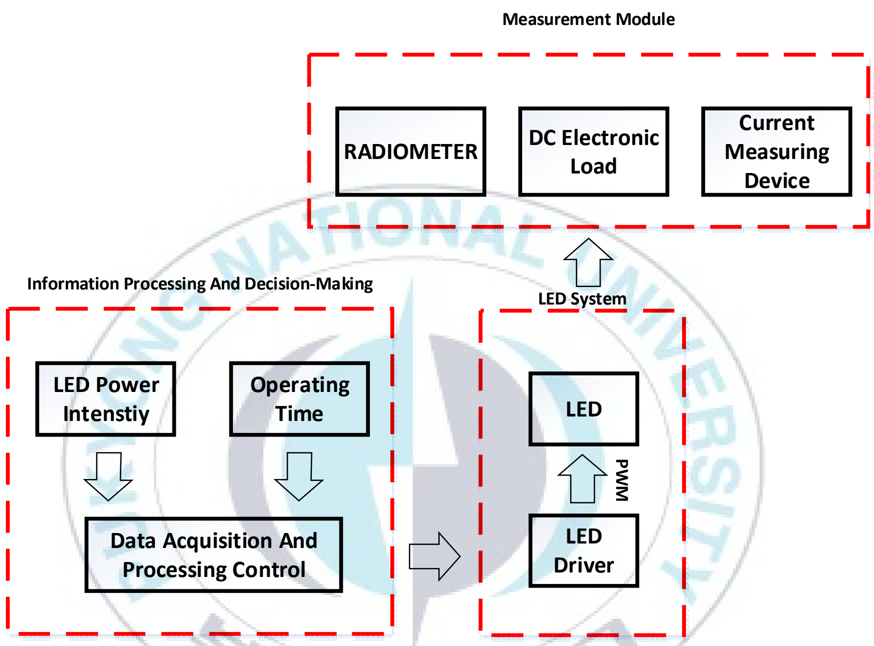

Figure 24 Block diagram of the LED Power Density control system.

1.1. Information Processing and Decision-Making

The information processing and the decision-making are two main units of this control system. The power density and operating time are inputs in information processing and decision-making. The data would be processed in data acquisition and processing control. Commands would be sent to LED drive to produce PWM for LED control. The main aim of the control system is to control constant LED power density.

1.2 LED system

The LED face mask consists of 180 LED. An 8 bits Digital to Analog Converter (DAC) is used for PWM regulation for each LED. The LED power density is controlled by adjusting the width of the 31,25 KHz cycle from 0 % to 99 %. The output current value is set by external resistor or programmed with using IREFALL register on LED driver.

1.3 Measurement Module

1.3.1. Light power density measurement

A laboratory radiometer (Biospherical Instruments Inc., USA) was used to measure light intensity. Photosynthesis photo flux density (PPFD; μ mol m^{-2} s^{-1}) was converted to radiant flux density (mW/cm^{-2}) by using the following formula [27]:

Radiant flux(W) = $h \times C \times NA \times PPDF$ (μ mol) / $\lambda \times 10^{(-3)}$, (1)

where, h is Plank constant ($6.626 \times (10)^{(-34)}$), C is light velocity ($3 \times 10^8$ $ms^{(-1)}$), λ is Wavelength (nm) and NA is Avogadro constant (6.023×10^{23}).

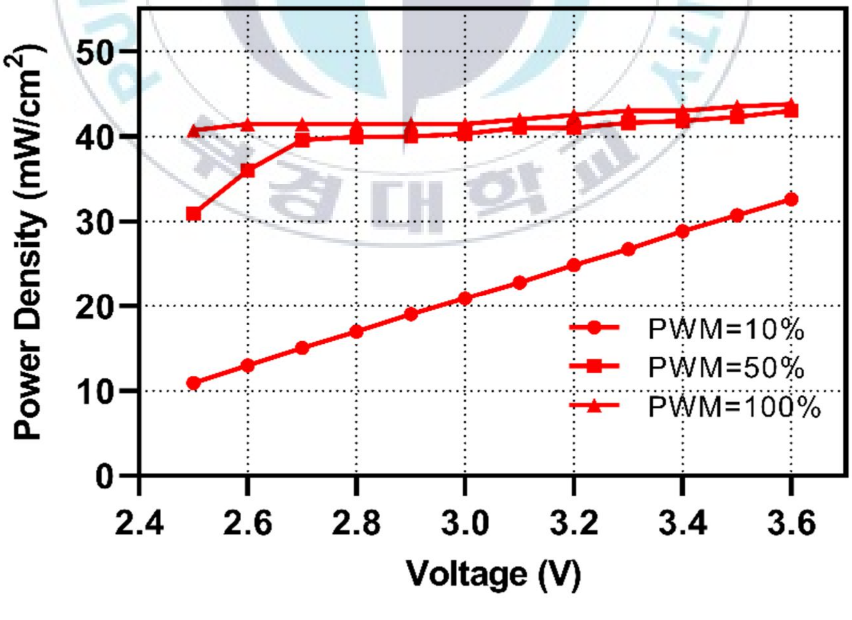

Figure 25 Power density of red light therapy with different LED voltage

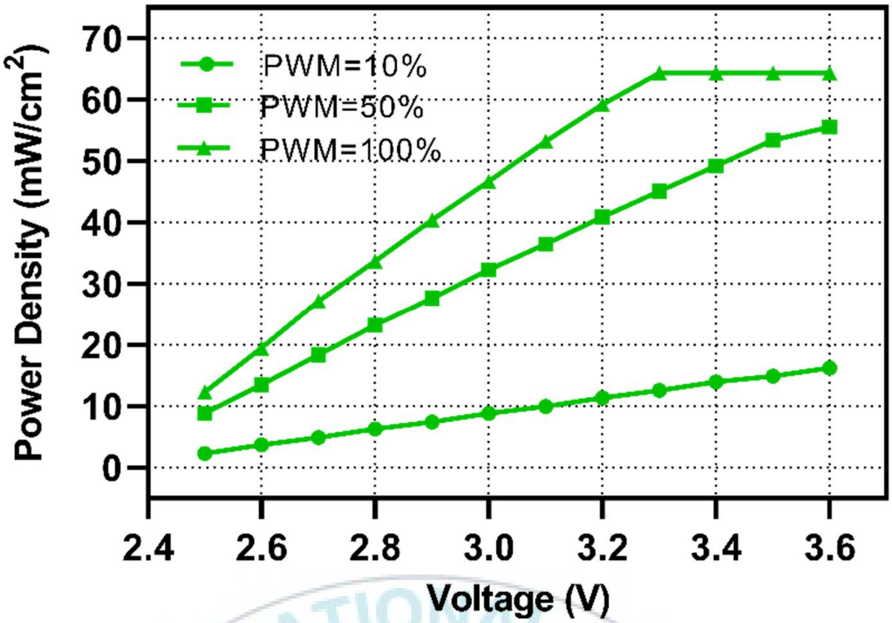

Figure 26 Power density of green light therapy with different LED voltage.

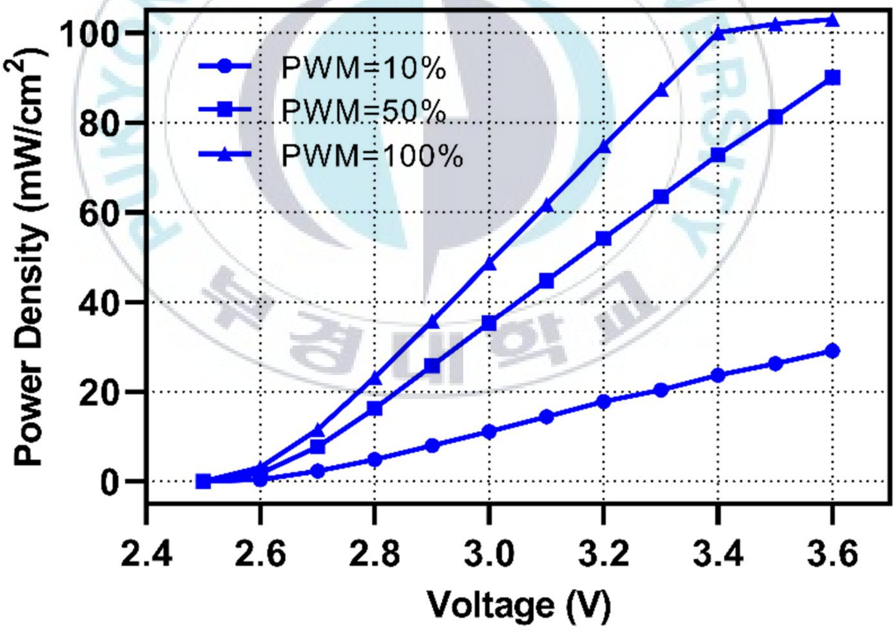

Figure 27 Power density of blue light therapy with different LED voltage.

The LED power source comes directly from a battery whose voltage would vary during discharging. Therefore, it is necessary to observe the relationship between LED power density with the decreased LED voltage. In this experiment, RIGOLDP832 was used to create different voltage and a laboratory radiometer was chosen to measure the power density of LED face mask with different PWM value.

To reduce the effect of daylight to the experimental result, all light intensity measurements were conducted in a dark room without any light source on. The influence of LED voltage on LED face mask power was shown in Fig. 25, Fig.26 and Fig. 27, respectively. These graphs indicate that LED power density changed in all group was voltage dependent and the decrease of battery voltage has caused a considerable decrease in LED power density. Futhermore, the power density test of the LED face mask revealed the LED power density at 100 % PWM value have a tendency to stay constant when LED reached maximum forward voltage.

1.4. Power Consumption and operating time

One major challenge in controlling LED power density is the attachment of radiometer or light sensor to the patient’s face in order to measure light power intensity and feedback to information processing and decision-making during phototherapy treatment. Therefore, in this design, we intended to develop a LED control system based on LED power density and the change of LED power

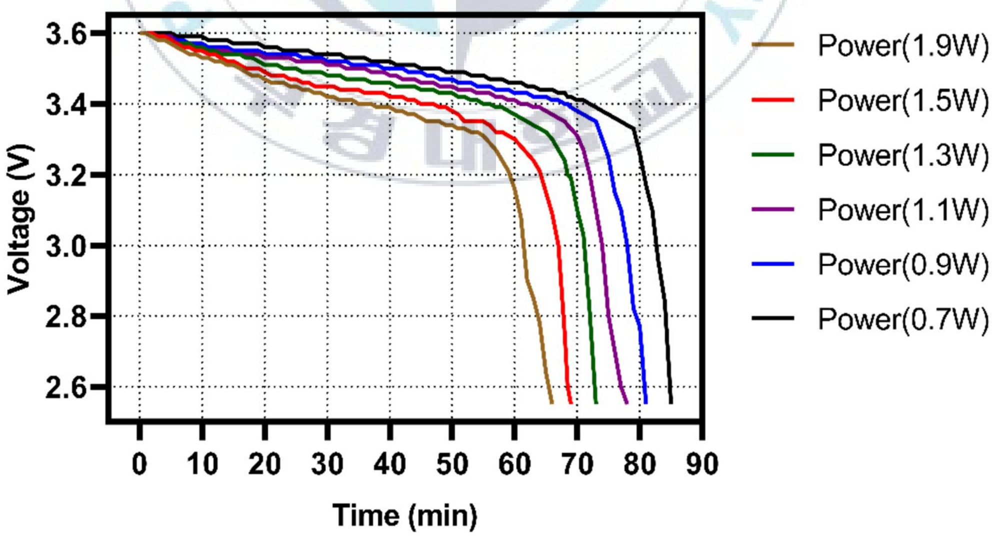

Figure 28 LED voltage with respect to operating time under different power consumption

M9712B-DC Electronic Load is used to test the operation of LED face mask battery with different constant power value. The battery expectant life curve and the battery voltage were measured and shown in Fig. 28. In this figure, the voltages of different power consumption tends to slightly decrease from 3.6 V to 3.3 V after 60 minutes for operation. It is also noticed that after the voltage reduced below 3.3, the battery voltage was dramatically decreased which affected the operating stability and reliability of LED face mask.

2. Designed Fuzzy Logic Controller

With the advantage of being robust and less requiring the extract mathematical model, Fuzzy logic controller is an appropriate tool for controlling LED power density [17-20].

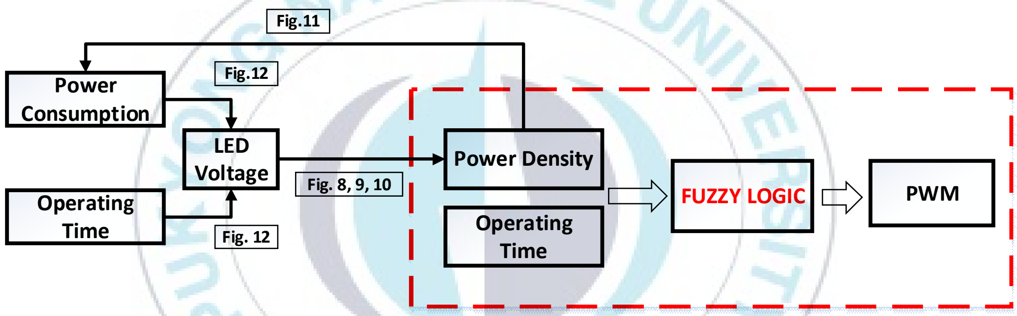

Figure 29 The structure of LED constant-power density control system

2.1. Fuzzification

In this work, the LED power density and used time are selected as the inputs of the Fuzzy logic conttroller and the PWM value is considered as the output of value.

Let, a1 = small (S), medium (M), large (L) for red LED, a2 = small-small (SS), small (S), medium (M), large (L), large-large (L-L) for blue LED and a3 = small-small (SS), small (S), medium (M), large (L), large-large (L-L) for green LED denote the domain of LED power density ranks. Each ranks depicted by a membership function, as shown in Fig.30.

Let, b = short-short (S-S), short (S), short-medium (S-M), medium (M), long (L) denote the domain of operating time ranks. Each rank is depicted by a membership function of trapezoid and triangular form, as shown in Fig. 30.

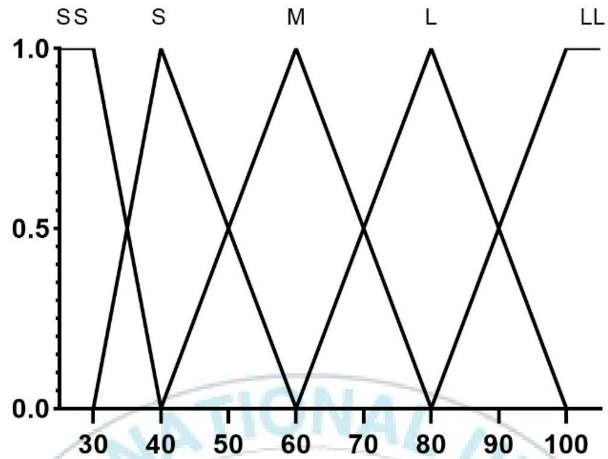

(a)

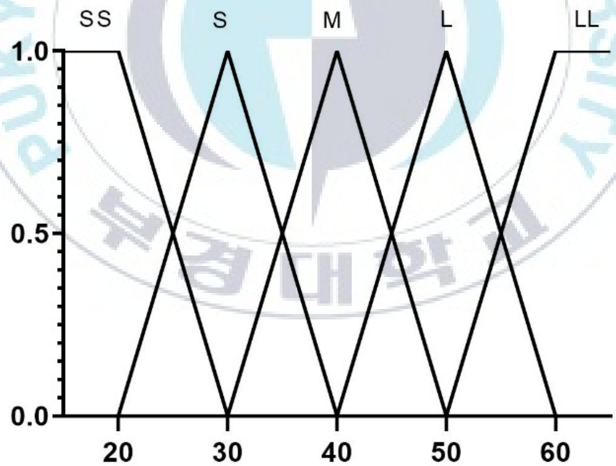

(b)

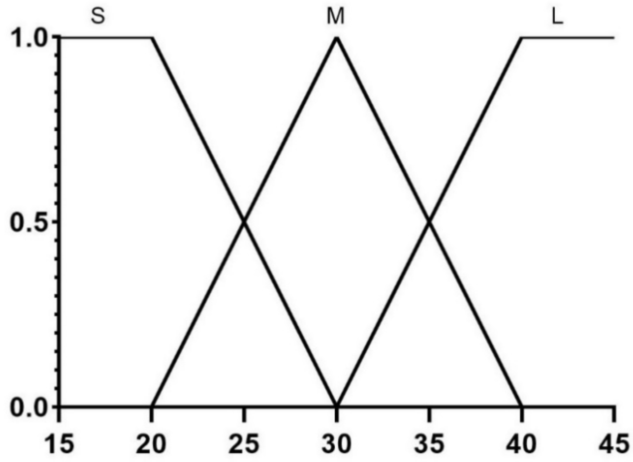

(c)

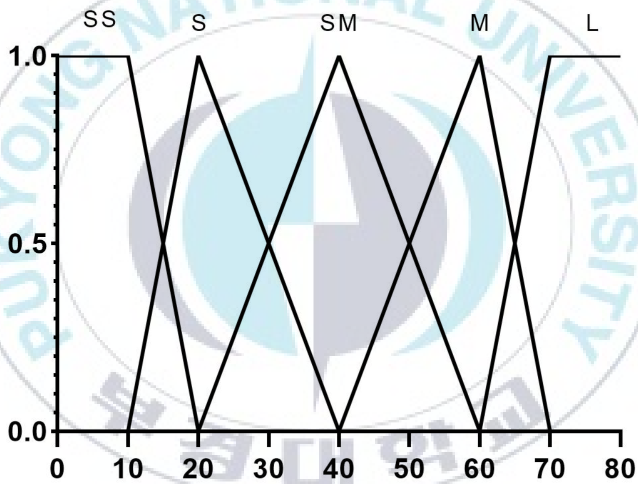

(d)

Figure 30 Membership functions: (a) Red LED power density; (b) Blue LED power density; (c) Green LED power density; (d) Operating time.

2.2. Interence Method

The rules for designing fuzzy logic controller was shown in Table 3, 4, 5, respectively, with each intersection of the row and column corresponds to a fuzzy rule. To operate the fuzzy combination, Sugeno's method with minimum (logical AND) in fuzzy logic and maximum (logical OR) in a set of fuzzy results was selected. A fuzzy system is a set of "if-then" rules that maps inputs to output [35]. A 3-D visualization of each inference rules was shown in Fig. 31, 32 and 33.

Table 6 Inference rules of Red Fuzzy logic controller

Time	Power Density		
	S	**M**	**L**
SS	5%	10%	50%
S	5%	10%	50%
SM	5%	15%	60%
M	10%	20%	None
L	10%	None	None

Table 7 Inference rules of Blue Fuzzy logic controller

Time	Power Density				
	SS	**S**	**M**	**L**	**LL**
SS	10%	15%	30%	50%	80%
S	10%	15%	30%	60%	100%
SM	15%	20%	40%	70%	100%
M	15%	25%	50%	None	None
L	20%	45%	None	None	None

Table 8 Inference rules of Green Fuzzy logic controller

Time	Power Density				
	SS	**S**	**M**	**L**	**LL**
SS	15%	25%	35%	45%	80%
S	15%	25%	40%	50%	80%
SM	20%	30%	40%	50%	85%
M	20%	35%	45%	60%	100%
L	25%	50%	None	None	None

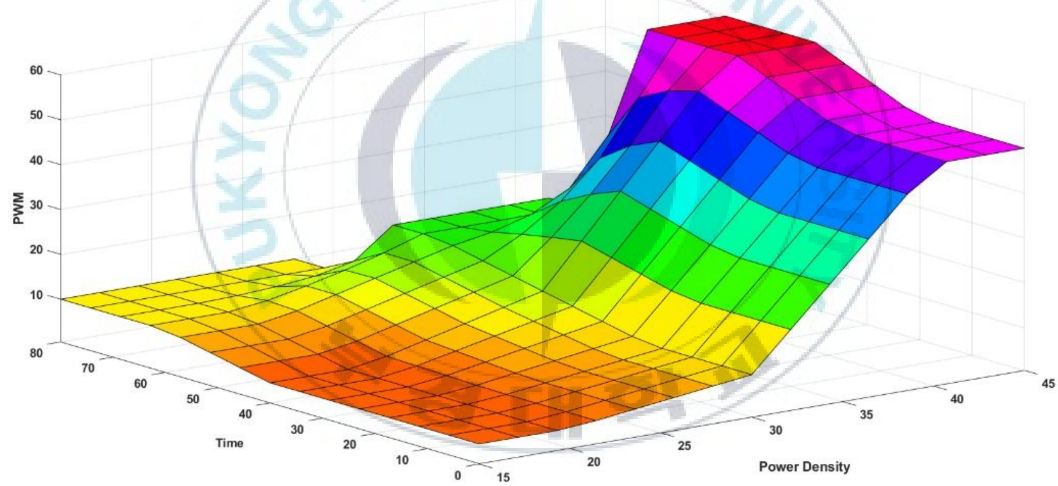

Figure 31 Fuzzy control surface for Red LED

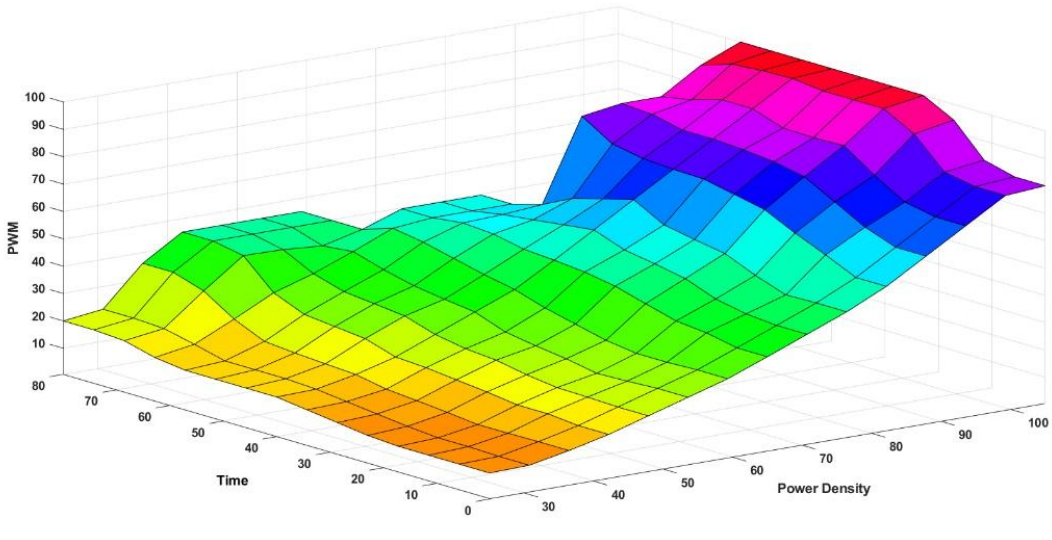

Figure 32 Fuzzy control surface for Blue LED

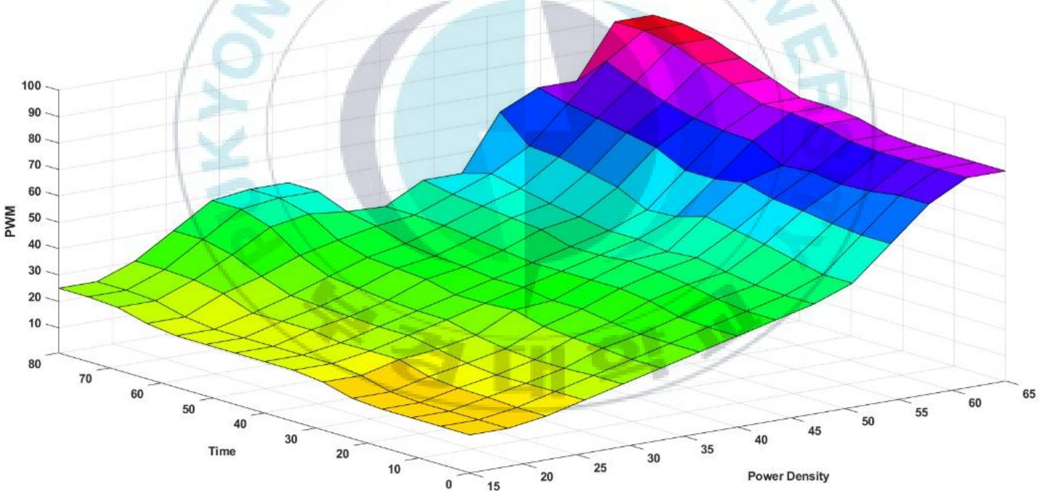

Figure 33 Fuzzy control surface for Green LED

2.3. Defuzzyfication

The last stage of the designed fuzzy logic controller is the defuzzification. Center of Gravity (COG) method was selected to transform the obtained fuzzy to a crisp value.

Chapter 4. EXPERIMENT WITH FUZZY LOGIC CONTROLLER

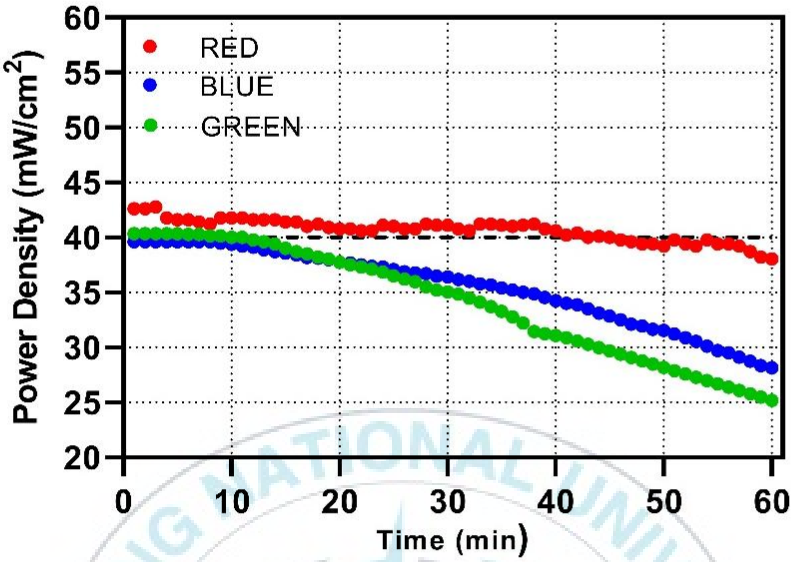

Figure 34 The power density of red, blue and green LED without the proposed control system. It is noted that the power density is set at 40 mW/cm^2

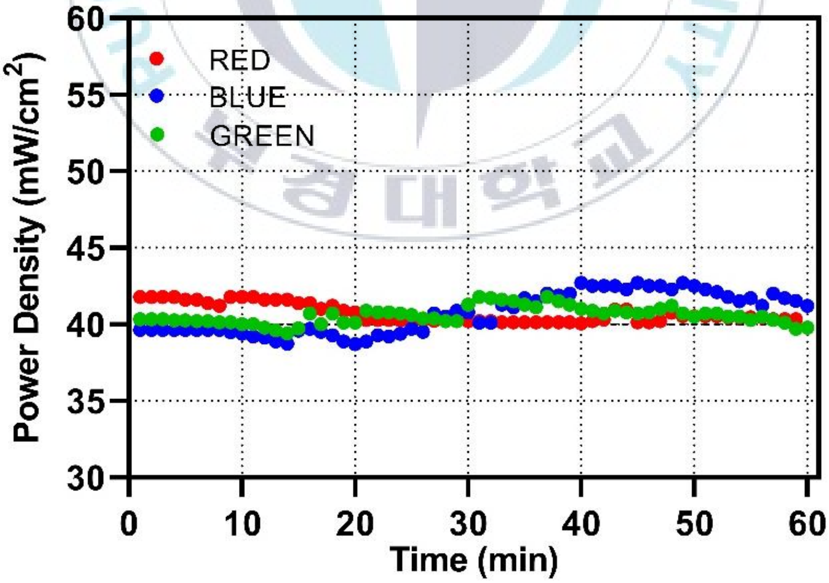

Figure 35 The power density of red, blue and green LED with the proposed control system. It is noted that the power density is set at 40 mW/cm2

The result of the open-loop LED control system design was analyzed and decrcibed in Fig. 34. The control system used the microprocessor PIC 16LF19186 as the central processing unit of the digital control system for command setting and controller calculation. The digital output was sent to LED driver (PCA9956) which regulated PWM applied to the LED to control power density. The power density through LED is measured using a radiometer.

In our present experimental design, we set 40 mW/cm^2 LED power density for LED face mask device [8-11, 28] .The power density of LED was measured at a fixed location with the same value for red, green, and blue experiment to test and analysis the control accuracy under battery voltage discharge. The evaluation results revealed that from 0 minute to 10 minute, the power density of LED face mask with and without controller was similar and remained constant due to the stable LED voltage. However, after 10 minutes, the value of blue and green power density without controller tends to gradually decrease (about 22% for green and 13% for blue at 40 minutes) and reduced rapidly until the lowest values were achieved, which were 25.17 mW/cm^2 for green and 28 mW/cm^2 for blue. While there was a slightly constant decline after 40 minute in red LED due to the high forward voltage of red LED, so the application of fuzzy controller is unnecessary to improve the setting power density in red LED. Regarding to the blue and green LED power density, the proposed controller have caused fluctuation in their values as shown in Fig.35. The measured values of green and blue LED power density are 40.57 mW/cm^2 and 40.71 mW/cm^2 with standard deviation of ± 0.558 mW/cm^2 and ± 1.329 mW/cm^2, respectively. In general, the result from measurements of red, green and blue power density indicated that the proposed system using Fuzzy logic controller is effective in robust change in LED voltage.

Chapter 5. CONCLUSION

In this paper, the design of the LED face mask with optimal power consumption and different LED color power density control was proposed and evaluated.

In power saving mode, the operating voltage of main component was seperated and functioned to lowest operating voltage to minimize current consumption. The consumed current of the LED face mask in power saving mode is lower than that in typical mode, which result in increasing the operating time of battery. The increase in the operating time of battery could lead to an improvement in operation and control accuracy in this proposed design. However, when waking-up from sleep mode, the MCU and Bluetooth modules need an extra delay time to return to the normal configuration showing some disadvantages in stabilizing of this design. The increased operation stability of MCU and Bluetooth module as well as enhanced the reliability of LED phototherapy system should be considered for further investigation.

Power density is an important parameter in phototherapy, as the stabilization of LED power intensity under large voltage variation is always necessary. The test results has shown the variation of LED voltage under recharging correspond to the change of LED power density. In this study, the relationship between LED power density, operating time and power consumption have been evaluated. A fuzzy controller was then proposed and designed for controlling constant – power density with an error of about 1.3 % , 3.3 %, 1.5 % for green, blue and red LED, respectively. The test data show that the proposed control system can provide a constant-LED power density under the variation of battery during recharge. This verifies the technical feasibility of proposed LED face mask and its application in phototherapy treatment.

References

[1] Leyden JJ. Therapy for acne vulgaris. New England Journal of Medicine. 1997;336:1156-62.

[2] Mulder M, Sigurdsson V, Van Zuuren E, Klaassen E, Faber J, De Wit J, et al. Psychosocial impact of acne vulgaris. Dermatology. 2001;203:124-30.

[3] Burton J, Cunliffe W, STAFFORD I, SHUSTER S. The prevalence of acne vulgaris in adolescence. British Journal of Dermatology. 1971;85:119-26.

[4] Pawin H, Beylot C, CHIVOT M, FAURE M, Florence P, REVUZ J, et al. Physiopathology of acne vulgaris: recent data, new understanding of the treatments. European Journal of Dermatology. 2004;14:4-12.

[5] Cooper AJ. Systematic review of Propionibacterium acnes resistance to systemic antibiotics. Medical journal of Australia. 1998;169:259-61.

[6] Feldman S, Careccia RE, Barham KL, Hancox J. Diagnosis and treatment of acne. American Family Physician. 2004;69:2123-38.

[7] Webster GF. Inflammation in acne vulgaris. Journal of the American Academy of Dermatology. 1995;33:247-53.

[8] Avci P, Gupta A, Sadasivam M, Vecchio D, Pam Z, Pam N, et al. Low-level laser (light) therapy (LLLT) in skin: stimulating, healing, restoring. Seminars in cutaneous medicine and surgery: NIH Public Access; 2013. p. 41.

[9] Lee W, Shalita AR, Poh-Fitzpatrick MB. Comparative studies of porphyrin production in Propionibacterium acnes and Propionibacterium granulosum. Journal of bacteriology. 1978;133:811-5.

[10] Goldberg DJ, Russell BA. Combination blue (415 nm) and red (633 nm) LED phototherapy in the treatment of mild to severe acne vulgaris. Journal of Cosmetic and Laser Therapy. 2006;8:71-5.

[11] Lee SY, You CE, Park MY. Blue and red light combination LED phototherapy for acne vulgaris in patients with skin phototype IV. Lasers in Surgery and Medicine: The Official Journal of the American Society for Laser Medicine and Surgery. 2007;39:180-8.

[12] MICROCHIP. PIC16LF19186. https://wwwmicrochipcom/wwwproducts/en/PIC16F19186.

[13] MICROCHIP. RN4020. https://wwwmicrochipcom/wwwproducts/en/RN4020. 2015.

[14] NXP. PCA9956. https://wwwnxpcom/docs/en/data-sheet/PCA9956Apdf. 2015.

[15] Bui NT, Vo TH, Kim B-G, Oh J. Design of a Solar-Powered Portable ECG Device with Optimal Power Consumption and High Accuracy Measurement. Applied Sciences. 2019;9:2129.
[16] Huang B-J, Chen C-W, Hsu P-C, Tseng W-M, Wu M-S. Direct battery-driven solar LED lighting using constant-power control. Solar Energy. 2012;86:3250-9.
[17] Yang C, Fan S, Wang Z, Li W. Application of fuzzy control method in a tunnel lighting system. Mathematical and Computer Modelling. 2011;54:931-7.
[18] Liu J, Zhang W, Chu X, Liu Y. Fuzzy logic controller for energy savings in a smart LED lighting system considering lighting comfort and daylight. Energy and Buildings. 2016;127:95-104.
[19] McAllister MN. Fuzzy logic with engineering applications (Timothy Ross). SIAM Review. 1996;38:174-5.
[20] Wang Z, Tan YK. Illumination control of LED systems based on neural network model and energy optimization algorithm. Energy and Buildings. 2013;62:514-21.
[21] Park D-H, Oh S-T, Lim J-H. Development of UVB LED Lighting System Based on UV Dose Calculation Algorithm to Meet Individual Daily UV Dose. Applied Sciences. 2019;9:2479.
[22] Park D-H, Oh S-T, Lim J-H. Development of a UV index sensor-based portable measurement device with the EUVB ratio of natural light. Sensors. 2019;19:754.
[23] Elektronik W. 5050 LED. https://katalogwe-onlinede/en/led/WL-SFTW. 2019.
[24] Intrument T. BQ24130. http://wwwticom/product/BQ24130. 2012.
[25] Instruments T. TPS763. http://wwwticom/lit/ds/symlink/tps763pdf. 2019.
[26] Instruments T. TPS61322. http://wwwticom/lit/ds/symlink/tps61322pdf. 2019.
[27] Roh HJ, Kim A, Kang GS, Kim D-H. Photoinactivation of major bacterial pathogens in aquaculture. Fisheries and Aquatic Sciences. 2016;19:28.
[28] Lam TS. Laser stimulation of collagen synthesis in human skin fibroblast cultures. Laser Life Science. 1986;1:61-77.

Acknowledgement

William Jennings Bryan said that " Destiny is no matter of chance. It is a matter of choice. It is not a thing to be waited for. It is a thing to be achieved". That's right. The more we grow up, the more decision and choice we have to make in our life. Sometime, I wonder about my life " in the thousand of decisions and choices, why we chose to belong together" and then, if destiny tried to arrange us together, we should appreciate that.

From deepest of my heart, I would like to express the biggest love to my family: my father, my mother and my young sister. They always beside me, always understand and let me know the value of my life. My family is my motivation to boost me to work hardly, put more effort in my life and more believing in myself. Thank to god, thank to destiny give me a chance to become a part of my family.

I would like to give my respect to my advisor Professor Junghwan Oh who are generous and kindest man with a warming heart. Thank you for everything you did to me. I believe that this time will be one of unforgettable time in my life. I wish the best for you and hopefully we can work together to make our dream come true.

Thanks to all of my lab mates who could be seen as my friends, my instructor and my family. I remember the first day when I came there. I could not image the life in Korea and what is going on. Thank for your kindly support, your help, which me stronger day by day. With me, it is more valuable than money or any jewelry. I wish one day you wish achieve your goals and make you dream come true.

Last word, I would like to send to warming message to my brothers, my sisters, my friends who I meet in PKNU and in "my group" . I know everyone I meet is for a reason. Thank to density to bring me to meet you who are always loving me. Thank for every valuable advices, thank for the time we can together.

Thank everyone to become a part of my life. Love you forever.

Phan Duc Tri